DESY 08-184
SFB/CPP-08-92
TTP08-50

DESY 08–184
SFB/CPP-08-92
TTP08–50

# Strong-Coupling Constant at Three Loops in Momentum Subtraction Scheme

K.G. Chetyrkin[a,b], B.A. Kniehl[c] and M. Steinhauser[a]

(a) Institut für Theoretische Teilchenphysik,
Universität Karlsruhe (TH), Karlsruhe Institute of Technology (KIT),
76128 Karlsruhe, Germany

(b) Institute for Nuclear Research, Russian Academy of Sciences,
Moscow 117312, Russia

(c) II. Institut für Theoretische Physik,
Universität Hamburg, 22761 Hamburg, Germany



**Abstract**

In this paper we compute the three-loop corrections to the $\beta$ function in a momentum subtraction (MOM) scheme with a massive quark. The calculation is performed in the background field formalism applying asymptotic expansions for small and large momenta. Special emphasis is devoted to the relation between the coupling constant in the MOM and $\overline{\rm MS}$ schemes as well as their ability to describe the phenomenon of decoupling.

It is demonstrated by an explicit comparison that the $\overline{\rm MS}$ scheme can be consistently used to relate the values of the MOM-scheme strong-coupling constant in the energy regions higher and lower than the massive-quark production threshold. This procedure obviates the necessity to know the full mass dependence of the MOM $\beta$ function and clearly demonstrates the equivalence of both schemes for the description of physics outside the threshold region.

PACS numbers: 12.38.-t, 12.38.Bx, 14.65.-q

# 1 Introduction

Within the perturbative framework, the $\overline{\rm MS}$ scheme [1, 2] based on dimensional regularization [3, 4, 5] is a well-established scheme for the renormalization of fields and parameters. This applies in particular to $\alpha_s$, the coupling constant of Quantum Chromodynamics (QCD). One of the major advantages of the $\overline{\rm MS}$ scheme is its simplicity in practical applications. The main reason for this is that it belongs to the class of so-called mass-independent schemes where the renormalization constants are independent of the precise configuration of masses and external momenta involved in the problem.

Within the $\overline{\rm MS}$ scheme, the beta function governing the running of $\alpha_s$ is know in the four-loop approximation [6, 7]. In order to correctly account for the heavy-quark thresholds, also the corresponding matching (or decoupling) conditions are needed, which allows for a precise relation of $\alpha_s$ at widely separated energy scales like, e.g., the tau lepton and $Z$ boson masses. Four-loop running goes along with three-loop matching, which is also known since more than ten years [8].[1]

Other renormalization schemes which do not have the nice property of mass-independence are significantly more complicated from the technical point of view — mainly because one has to deal with Feynman integrals involving many mass scales. Still, at the level of precision which has been reached in the recent years, it is necessary to have a cross check of the dependence on the renormalization scheme. In this paper, we want to provide an alternative set-up to the running and decoupling of $\alpha_s$ in the $\overline{\rm MS}$ scheme and consider a momentum subtraction (MOM) scheme for the definition of $\alpha_s$. We will provide $\overline{\rm MS}$ to MOM conversion formulae and the MOM beta function in the three-loop order and are thus able to cross check the $\overline{\rm MS}$ running of $\alpha_s$. A two-loop analysis has been performed in Ref. [11]. In this paper we check the calculation of Ref. [11] and extend the analysis to three loops.

The remainder of the paper is organized as follows: In the next section, we describe our setup. In particular, we derive the relation between the strong coupling in the $\overline{\rm MS}$ scheme and in two versions of the momentum subtraction scheme and provide the corresponding beta functions. In Section 3, we present our analytical results for the gluon polarization function in the background field formalism and discuss the phenomenological applications in Section 4, where we compare the running in the $\overline{\rm MS}$ and MOM schemes. Our conclusions are summarized in Section 5.

# 2 The strong coupling in the MOM scheme

For convenience, we adopt Landau gauge, which has the advantage that the renormalization group equations for the gauge parameter and $\alpha_s$ decouple. Furthermore, we require that the polarization function of the gluon vanishes for $Q^2 \equiv -q^2 = \mu^2 > 0$.

For the practical calculation, we adopt the background field gauge [12], which has the nice feature that the $\beta$ function of the strong coupling is determined from the gluon

[1] Recently, also the four-loop decoupling constants have been computed [9, 10].

polarization function alone. The latter is given by

$$\Pi^{\mu\nu}(q) \;=\; \left(-g^{\mu\nu}q^2 + q^\mu q^\nu\right)\Pi(q^2)\,, \tag{1}$$

which is conveniently decomposed as follows

$$\Pi(q^2) \;=\; \sum_{i\geq 1}\Pi^{(i)}(q^2,\mu^2,\{M_Q^2\})\left(\frac{\alpha_s}{\pi}\right)^i\,. \tag{2}$$

In the $i$-loop contribution, the dependence on $q$, $\mu$ and the various quark masses is explicitly displayed. Formulae (1) and (2) hold both in the $\overline{\rm MS}$ and MOM schemes. The corresponding functions, $\Pi(q^2)$ and $\Pi^{\rm MOM}(q^2)$, can be used to obtain a relation between $\alpha_s$ and $\alpha_s^{\rm MOM}$, the strong couplings in the $\overline{\rm MS}$ and MOM schemes, using the fundamental concept of the *invariant charge* [13, 14]:

$$\frac{\alpha_s^{\rm MOM}(\mu^2)}{1+\Pi^{\rm MOM}(q^2)} = \frac{\alpha_s(\mu^2)}{1+\Pi(q^2)}\,. \tag{3}$$

It is an important and unique feature of the background field gauge that the invariant charge is expressible in terms of the coupling constant and the gluon polarization operator *only* in exactly the same simple way as in QED. We define $\Pi^{\rm MOM}(q^2)$ such that $\Pi^{\rm MOM}(-\mu^2)=0$ and, consequently, we have

$$\begin{aligned}
\alpha_s^{\rm MOM}(\mu^2) &= \alpha_s^{(n_f)}(\mu^2)\left[1 + c_1\frac{\alpha_s^{(n_f)}(\mu^2)}{\pi} + c_2\left(\frac{\alpha_s^{(n_f)}(\mu^2)}{\pi}\right)^2 + c_3\left(\frac{\alpha_s^{(n_f)}(\mu^2)}{\pi}\right)^3\right]\,,\\
c_1 &= -\Pi_0^{(1)},\\
c_2 &= -\Pi_0^{(2)} + \left(\Pi_0^{(1)}\right)^2,\\
c_3 &= -\Pi_0^{(3)} + 2\Pi_0^{(1)}\Pi_0^{(2)} - \left(\Pi_0^{(1)}\right)^3\,,
\end{aligned} \tag{4}$$

where $\Pi_0^{(i)} = \Pi^{(i)}(-\mu^2)$ has been introduced. It is instructive to look at the explicit expressions in the massless limit with $n_f = n_l$ massless quarks. In this case, we obtain

$$\begin{aligned}
\alpha_s^{\rm MOM}(\mu^2) \;=\; & \alpha_s^{(n_l)}(\mu^2)\Bigg[1 + \frac{\alpha_s^{(n_l)}(\mu^2)}{4\pi}\left(\frac{205}{12} - \frac{10}{9}n_l\right) + \left(\frac{\alpha_s^{(n_l)}(\mu^2)}{4\pi}\right)^2\left(\frac{90391}{144}\right.\\
& \left. - \frac{513}{8}\zeta(3) + \left(-\frac{2066}{27} - \frac{4}{3}\zeta(3)\right)n_l + \frac{100}{81}n_l^2\right)\\
& + \left(\frac{\alpha_s^{(n_l)}(\mu^2)}{4\pi}\right)^3\left(\frac{50765707}{1728} - \frac{23343}{4}\zeta(3) - \frac{24885}{64}\zeta(5) + \left(-\frac{860917}{162}\right.\right.\\
& \left.\left. + \frac{20423}{54}\zeta(3) + \frac{2320}{9}\zeta(5)\right)n_l + \left(\frac{209407}{972} + \frac{28}{9}\zeta(3)\right)n_l^2 - \frac{1000}{729}n_l^3\right)\Bigg]\,.
\end{aligned} \tag{5}$$

In analogy to the $\overline{\rm MS}$ scheme, the $\beta$ function in the MOM scheme is defined through

$$\mu^2 \frac{\rm d}{{\rm d}\mu^2} \frac{\alpha_s^{\rm MOM}}{\pi} = \beta^{\rm MOM}(\alpha_s^{\rm MOM}) = -\left(\frac{\alpha_s^{\rm MOM}}{\pi}\right)^2 \sum_{i\geq 0} \beta_i^{\rm MOM} \left(\frac{\alpha_s^{\rm MOM}}{\pi}\right)^i , \qquad (6)$$

where — in contrast to the $\overline{\rm MS}$ scheme — the coefficients $\beta_i^{\rm MOM}$ are functions of the renormalization scale $\mu$ and the quark masses. With the help of Eq. (3), where we replace on the right-hand side the $\overline{\rm MS}$ renormalized quantities by the bare ones, it is possible to obtain a relation between $\beta^{\rm MOM}$ and the coefficients $\Pi^{(i),{\rm MOM}} = \Pi^{(i),{\rm MOM}}(q^2, \mu^2, \{M_Q^2\})$, which reads

$$\beta^{\rm MOM}(\alpha_s^{\rm MOM}) = \frac{\alpha_s^{\rm MOM}}{\pi} \frac{\sum_{i\geq 1} \left(\frac{\alpha_s^{\rm MOM}}{\pi}\right)^i \mu^2 \frac{\rm d}{{\rm d}\mu^2} \Pi^{(i),{\rm MOM}}}{1 - \sum_{i\geq 1} (i-1) \left(\frac{\alpha_s^{\rm MOM}}{\pi}\right)^i \Pi^{(i),{\rm MOM}}} . \qquad (7)$$

From this equation, one can easily derive convenient formulae for $\beta_i^{\rm MOM}$. Note that the term in the denominator of Eq. (7) contributes for the first time at the three-loop order. Let us also mention that, starting at this order, a non-trivial $q^2$ dependence occurs on the right-hand side of Eq. (7) which has to cancel in the proper combination of the $\Pi^{(i),{\rm MOM}}$ functions.

The functions $\beta_0^{\rm MOM}$ and $\beta_1^{\rm MOM}$ are known analytically [11]. The three-loop contribution $\beta_2^{\rm MOM}$ is evaluated in the asymptotic regions for large and small quark masses analytically in this paper. An approximate formula valid for arbitrary quark masses is easily obtained by interpolation between the low- and high-energy regions.

In the massless limit, the first three coefficients are given by

$$\begin{aligned}
\beta_{0,\rm ml}^{\rm MOM} &= \frac{1}{4}\left[\frac{11}{3} C_A - \frac{4}{3} T n_l\right] , \\
\beta_{1,\rm ml}^{\rm MOM} &= \frac{1}{16}\left[\frac{34}{3} C_A^2 - \frac{20}{3} C_A T n_l - 4 C_F T n_l\right] , \\
\beta_{2,\rm ml}^{\rm MOM} &= \frac{1}{64}\left[-\left(-\frac{3005}{24} + \frac{209}{8}\zeta(3)\right) C_A^3 - \left(\frac{1861}{18} + \frac{119}{6}\zeta(3)\right) C_A^2 T n_l \right. \\
&\quad - \left(\frac{605}{9} - \frac{176}{3}\zeta(3)\right) C_A C_F T n_l - \left(-\frac{130}{9} - \frac{32}{3}\zeta(3)\right) C_A T^2 n_l^2 \\
&\quad \left. - \left(-\frac{184}{9} + \frac{64}{3}\zeta(3)\right) C_F T^2 n_l^2 + 2 C_F^2 T n_l\right] ,
\end{aligned} \qquad (8)$$

where $C_A = 3, C_F = 4/3, T = 1/2$ and $n_l$ is the number of massless quarks. Since the first two coefficients of the $\beta$ function are scheme independent $\beta_{0,\rm ml}^{\rm MOM}$ and $\beta_{1,\rm ml}^{\rm MOM}$ coincide with their counterparts in the $\overline{\rm MS}$ scheme. $\beta_{2,\rm ml}^{\rm MOM}$, however, differs from its $\overline{\rm MS}$ counterpart [15, 16]. It is worthwhile to mention that $\beta_{2,\rm ml}^{\rm MOM}$ contains the Riemann $\zeta$ function $\zeta(3)$, which in the $\overline{\rm MS}$ scheme only appears at the four-loop order.

The three-loop results in Eqs. (5) and (8) are new, and the two-loop expressions are in agreement with Ref. [11].

The practical evaluation of $\Pi^{\rm MOM}(q^2)$ entering the equation for the beta function can be reduced to the evaluation of $\Pi(q^2)$ in the $\overline{\rm MS}$ scheme. The corresponding relation is obtained from Eq. (3), this time for arbitrary values of $q^2$ and $\mu^2$, which can be solved for $\Pi^{\rm MOM}$. After properly replacing $\alpha_s^{\rm MOM}$ by $\alpha_s$ using Eq. (4), one gets (the dependence on the quark masses is suppressed)

$$\begin{aligned}
\Pi^{(1),{\rm MOM}}(q^2) &= \Pi^{(1)}(q^2) - \Pi_0^{(1)} \,, \\
\Pi^{(2),{\rm MOM}}(q^2) &= \Pi^{(2)}(q^2) - \Pi_0^{(2)} \,, \\
\Pi^{(3),{\rm MOM}}(q^2) &= \Pi^{(3)}(q^2) - \Pi_0^{(3)} + \Pi_0^{(1)} \left( \Pi^{(2)}(q^2) - \Pi_0^{(2)} \right) \,,
\end{aligned} \tag{9}$$

where $\Pi_0^{(i)}$ is defined below Eq. (4). Note, that by construction we have $\Pi^{\rm MOM}(-\mu^2) = 0$.

The polarization function in the $\overline{\rm MS}$ scheme is obtained in the standard way by renormalizing $\alpha_s$ in the $\overline{\rm MS}$ scheme, the quark masses in the on-shell scheme and taking care of the gluon wave function renormalization.

In Ref. [11], it has been observed that there are relatively large coefficients in the relation between $\alpha_s$ and $\alpha_s^{\rm MOM}$ when running from $\alpha_s(M_Z)$ down to, say, $\alpha_s(M_\tau)$. The situation was improved in Ref. [11] by a simple trick of rescaling the scale parameter $\mu$. Let us start from the massless limit corresponding to $\mu \gg M_t$. In this case, relation (5) assumes the form

$$\begin{aligned}
\alpha_s^{\rm MOM}(\mu^2) &= \alpha_s^{(6)}(\mu^2) \left[ 1 + 10.417 \, \frac{\alpha_s^{(6)}(\mu^2)}{4\pi} + 126.350 \, \left( \frac{\alpha_s^{(6)}(\mu^2)}{4\pi} \right)^2 \right. \\
&\quad \left. + 2000.062 \, \left( \frac{\alpha_s^{(6)}(\mu^2)}{4\pi} \right)^3 \right] .
\end{aligned} \tag{10}$$

In a next step, we introduce a new, rescaled MOM scheme with the help of

$$\alpha_s^{\overline{\rm MOM}}(\mu^2) \equiv \alpha_s^{\rm MOM}(x_0^2 \mu^2) \tag{11}$$

or, equivalently (with $L = \ln(x_0^2)$),

$$\begin{aligned}
\alpha_s^{\overline{\rm MOM}} &\equiv \alpha_s^{\rm MOM} \left[ 1 + r_1 \frac{\alpha_s^{\rm MOM}}{\pi} + r_2 \left( \frac{\alpha_s^{\rm MOM}}{\pi} \right)^2 + r_3 \left( \frac{\alpha_s^{\rm MOM}}{\pi} \right)^3 \right] \,, \\
r_1 &= -L \beta_{0,{\rm ml}}^{\rm MOM} \,, \\
r_2 &= \left( L \beta_{0,{\rm ml}}^{\rm MOM} \right)^2 - L \beta_{1,{\rm ml}}^{\rm MOM} \,, \\
r_3 &= \frac{5}{2} L^2 \beta_{0,{\rm ml}}^{\rm MOM} \beta_{1,{\rm ml}}^{\rm MOM} - L \beta_{2,{\rm ml}}^{\rm MOM} - \left( L \beta_{0,{\rm ml}}^{\rm MOM} \right)^3 \,,
\end{aligned} \tag{12}$$

where $\beta_{i,\rm ml}^{\rm MOM}$ are given in Eq. (8). The corresponding generalization of Eq. (4) reads:

$$\begin{aligned}
\alpha_s^{\overline{\rm MOM}}(\mu^2) &= \alpha_s^{(n_f)}(\mu^2)\left[1+\overline{c}_1\frac{\alpha_s^{(n_f)}(\mu^2)}{\pi}+\overline{c}_2\left(\frac{\alpha_s^{(n_f)}(\mu^2)}{\pi}\right)^2+\overline{c}_3\left(\frac{\alpha_s^{(n_f)}(\mu^2)}{\pi}\right)^3\right], \\
\overline{c}_1 &= r_1-\Pi_0^{(1)}, \\
\overline{c}_2 &= -\Pi_0^{(2)}+\left(\Pi_0^{(1)}\right)^2-2\,\Pi_0^{(1)}\,r_1+r_2, \\
\overline{c}_3 &= -\Pi_0^{(3)}+2\Pi_0^{(1)}\Pi_0^{(2)}-\left(\Pi_0^{(1)}\right)^3+3\left(\Pi_0^{(1)}\right)^2 r_1 \\
&\quad -2\Pi_0^{(2)}r_1-3\;\Pi_0^{(1)}\,r_2+r_3\,. \qquad (13)
\end{aligned}$$

In a next step, following Ref. [11], we *tune* the parameter $x_0$ so that the difference between $\alpha_s^{\overline{\rm MOM}}$ and $\alpha_s^{(6)}$ starts only in order $\alpha_s^2$. The result reads[2]

$$\ln(x_0^2) = \frac{125}{84}\,, \qquad x_0\approx 2.1044\,, \qquad (14)$$

which leads to

$$\begin{aligned}
r_1 &\approx -2.60417\,, \\
r_2 &\approx 4.3635\,, \\
r_3 &\approx 2.2313\,. \qquad (15)
\end{aligned}$$

It is instructive to look again at the relation between $\alpha_s^{\overline{\rm MOM}}$ and $\alpha_s^{(6)}$ for $\mu \gg M_t$, which is now given by

$$\alpha_s^{\overline{\rm MOM}}(\mu^2) = \alpha_s^{(6)}(\mu^2)\left\{1+\tilde{k}_1\frac{\alpha_s^{(6)}(\mu^2)}{4\pi}+\tilde{k}_2\left(\frac{\alpha_s^{(6)}(\mu^2)}{4\pi}\right)^2+\tilde{k}_3\left(\frac{\alpha_s^{(6)}(\mu^2)}{4\pi}\right)^3\right\}, \qquad (16)$$

where

$$\begin{aligned}
\tilde{k}_1 &= 0, \\
\tilde{k}_2 &= \frac{11063}{168}-\frac{577}{8}\zeta(3) \approx -20.8472\,, \\
\tilde{k}_3 &= \frac{101389}{126}-\frac{345779}{288}\zeta(3)+\frac{222305}{192}\zeta(5) \approx 562.0541\,. \qquad (17)
\end{aligned}$$

As compared to Eq. (10), we observe a significant reduction in the magnitude of the coefficients in the rescaled relation (16), both at the two- and three-loop orders.[3] Furthermore,

[2]Note that there seems to be a misprint in the numerical value of $x_0$ quoted in Ref. [11], however, in the caption of Fig. 4 therein it is correct.

[3]Note that our value for the two-loop coefficient in Eq. (16) ($-20.8472$) differs from the one obtained in Ref. [11] ($-32.46$).

there is a different sign in the three-loop coefficient as compared to the two-loop one, which points to a better convergence of the perturbative expansion.

In the massless limit, both definitions for $\alpha_s^{\overline{\rm MOM}}(\mu^2)$, namely Eqs. (11) and (12), are completely equivalent. Following again Ref. [11], we choose Eq. (12) as the proper definition of the $\alpha_s^{\overline{\rm MOM}}(\mu^2)$ for *all* values of $\mu$. This choice has the advantage that the thresholds in the corresponding function $\beta^{\overline{\rm MOM}}$ remain "physical", that is located at $-\mu^2 = 4M_Q^2$. This follows directly from the relation between both $\beta$ functions:

$$\begin{aligned}
\beta_0^{\overline{\rm MOM}} &= \beta_0^{\rm MOM}\,, \\
\beta_1^{\overline{\rm MOM}} &= \beta_1^{\rm MOM}\,, \\
\beta_2^{\overline{\rm MOM}} &= \beta_2^{\rm MOM} - r_1\beta_1^{\rm MOM} + \left(r_2 - r_1^2\right)\beta_0^{\rm MOM}\,.
\end{aligned} \tag{18}$$

It is interesting to remark that the rescaling procedure significantly improves the $\overline{\rm MOM}$ to $\overline{\rm MS}$ relations also for moderate and even rather low values of $\mu$ (see below).

In the applications of Section 4, we consider the strong coupling both for energy scales of the order of or larger than and for those significantly smaller than the top-quark mass. In the latter case, we construct different MOM and $\overline{\rm MOM}$ schemes, which are derived from the choice $n_f = 5$ as the massless limit. In this case, we obtain the values

$$\begin{aligned}
x_0 &= e^{415/552} \approx 2.1208\,, \\
\tilde{k}_2 &= \frac{140689}{1656} - \frac{1699}{24}\zeta(3) \approx -0.1385\,, \\
\tilde{k}_3 &= \frac{143409281}{89424} - \frac{1225793}{864}\zeta(3) + \frac{518435}{576}\zeta(5) \approx 831.5896\,, \\
r_1 &= -\frac{415}{144} \approx -2.8819\,, \\
r_2 &= \frac{2228135}{476928} \approx 4.6719\,, \\
r_3 &= -\frac{1188703175}{68677632} + \frac{705085}{55296}\zeta(3) \approx -1.9809\,.
\end{aligned} \tag{19}$$

The same comments and conclusions hold as for $n_f = 6$.

# 3 Results

Let us in a first step briefly describe the evaluation of the gluon polarization function up to three loops within the background field formalism involving heavy quarks with generic mass $M_Q$. The basic idea is to evaluate $\Pi(q^2)$ for large and small external momenta and to obtain an approximation for all values of $q^2/M_Q^2$ by a simple interpolation procedure. Note that in our case the external momentum is space-like so that there are no problems with particle thresholds. Up to the two-loop order, only one quark flavour can occur in a diagram. At three loops, there are diagrams with a second closed fermion loop so that in principle a further mass scale can occur (see, e.g., the diagram in Fig. 1(g)). However, we

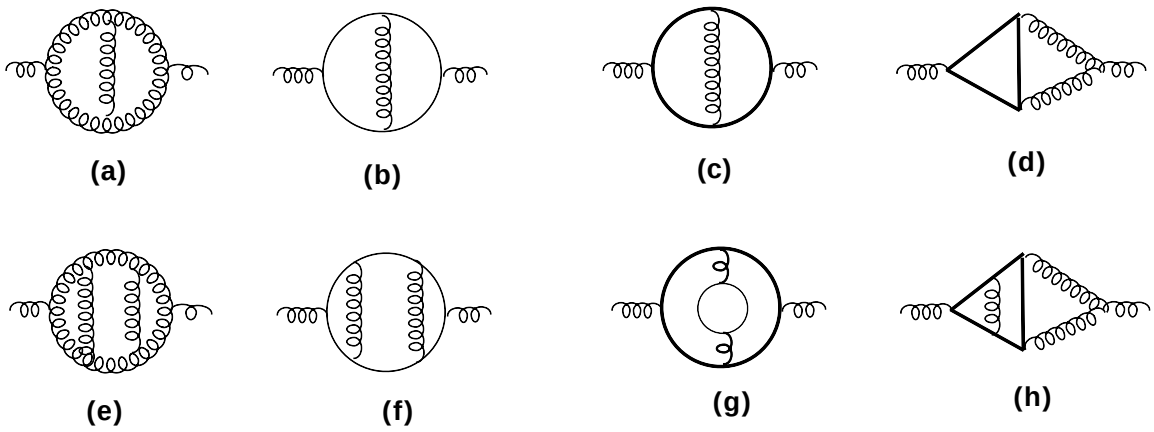


Figure 1: Sample diagrams contributing to the gluon propagator in the background field formalism at the two- and three-loop orders. Diagrams (a), (b), (e) and (f) only contain massless lines, while the others also contain massive ones due to the presence of the heavy-quark loop (thick line). (We have used the package `JaxoDraw` [17, 18] to draw the diagrams.)

assume a strong hierarchy in the quark masses such that we can always neglect the lighter mass. Thus, in this section, we consider QCD with total number $n_f$ of quark flavours. One quark, $Q$, has the (pole) mass $M_Q$, and all other $n_l = n_f - 1$ quarks are considered as massless.

As mentioned above, the $\overline{\rm MS}$ renormalized polarization function is needed in Landau gauge. However, in our calculation we adopt a general gauge parameter $\xi$ since the complexity is comparable to Landau gauge.

Some sample diagrams for $\Pi(q^2)$ are shown in Fig. 1. The diagrams are divided into two classes: completely massless diagrams and and diagrams involving massive-quark loops. The only scale in the massless diagrams is the external momentum. Thus they can be evaluated using `MINCER` [19, 20]. In the second class, the mass of the heavy quark sets another scale which makes the calculation significantly more difficult. The one- and two-loop calculations can be performed analytically, and the results can be found in Ref. [11]. At the three-loop order, however, an exact calculation is not yet possible. We perform an asymptotic expansion in the limits $q^2 \ll M_Q^2$ and $q^2 \gg M_Q^2$. Note that due to the diagrams containing massive-quark loops along with massless cuts (see, e.g., Figs. 1(d) and (h)) also the small-$q^2$ expansion turns out to be nontrivial. As a result, one encounters $\ln(q^2/M_Q^2)$ terms also in this limit.

All Feynman diagrams are generated with `QGRAF` [21]. The various diagram topologies are identified and transformed to `FORM` [22] with the help of `q2e` and `exp` [23, 24]. The program `exp` is also used in order to apply the asymptotic expansion (see, e.g., Ref. [25]) in the various mass hierarchies. The actual evaluation of the integrals is performed with the packages `MATAD` [26] and `MINCER` [20], resulting in an expansion in $d - 4$ for each

diagram, where $d$ is the space-time dimension.

We computed four expansion terms for small and six terms for large external momentum. In the following, we present only the leading and subleading terms of the corresponding expansions for the gluon polarization operator and the MOM $\beta$ function for $\mu^2 = Q^2$ and provide the complete expressions in a `Mathematica` file.[4] For completeness, we also list the one- and two-loop results, which agree with the corresponding expansions of the exact expressions [11]. It is convenient to cast the result in the form

$$\Pi(q^2) = \Pi^{\rm ml}(q^2) + \Pi^{\rm mv}(q^2, M_Q^2)\,, \tag{20}$$

and introduce the variable

$$Z = \frac{Q^2}{4M_Q^2}\,. \tag{21}$$

The results for the massless $\overline{\rm MS}$ renormalized polarization function reads

$$\begin{aligned}
\Pi_0^{(1),{\rm ml}} &= -\frac{205}{48} + n_l\frac{5}{18}\,,\\
\Pi_0^{(2),{\rm ml}} &= -\frac{2687}{128} + \frac{513}{128}\zeta(3) + n_l\left(\frac{347}{144} + \frac{1}{12}\zeta(3)\right)\,,\\
\Pi_0^{(3),{\rm ml}} &= -\frac{413343}{2048} + \frac{58317}{1024}\zeta(3) + \frac{24885}{4096}\zeta(5) + n_l\left(\frac{1476013}{41472} - \frac{3797}{864}\zeta(3) - \frac{145}{36}\zeta(5)\right)\\
&\quad + n_l^2\left(-\frac{64627}{62208} - \frac{1}{432}\zeta(3)\right)\,.
\end{aligned} \tag{22}$$

In the limit $Z \to 0$, we get

$$\begin{aligned}
\Pi_0^{(1),{\rm mv}} &= \frac{1}{6}\ln(4Z) - \frac{2}{15}Z + \mathcal{O}(Z^2)\,,\\
\Pi_0^{(2),{\rm mv}} &= \frac{7}{24} + \frac{19}{24}\ln(4Z) + \left(\frac{50239}{97200} - \frac{7}{15}\ln(4Z)\right)Z + \mathcal{O}(Z^2)\,,\\
\Pi_0^{(3),{\rm mv}} &= \frac{58933}{124416} + \left(\frac{2}{3} + \frac{2}{9}\ln 2\right)\zeta(2) + \frac{80507}{27648}\zeta(3) + \ln(4Z)\left(\frac{58939}{6912} - \frac{171}{256}\zeta(3)\right)\\
&\quad + \frac{283}{576}\ln^2(4Z) + n_l\left[-\frac{2479}{31104} - \frac{1}{9}\zeta(2) + \ln(4Z)\left(-\frac{1103}{1728} - \frac{1}{72}\zeta(3)\right)\right]\\
&\quad + Z\left\{\frac{6252381359}{279936000} + \frac{495461}{2332800}\ln(4Z) - \frac{6403}{4608}\ln^2(4Z) - \frac{8}{15}\zeta(2)\right.\\
&\quad -\frac{8}{45}\zeta(2)\ln 2 - \frac{625415}{31104}\zeta(3) + n_l\left[-\frac{118427}{291600} + \frac{12401}{58320}\ln(4Z)\right.\\
&\quad \left.\left.+\frac{61}{2592}\ln^2(4Z) + \frac{4}{45}\zeta(2)\right]\right\} + \mathcal{O}(Z^2)\,,
\end{aligned} \tag{23}$$

[4] See `http://www-ttp.particle.uni-karlsruhe.de/Progdata/ttp08/ttp08-50`.

and in the large-$Z$ region, we obtain

$$
\begin{aligned}
\Pi_0^{(1),\mathrm{mv}} &= \frac{5}{18} - \frac{1}{4Z} + \mathcal{O}\left(\frac{1}{Z^2}\right) , \\
\Pi_0^{(2),\mathrm{mv}} &= \frac{347}{144} + \frac{1}{12}\zeta(3) - \frac{1}{Z}\left(\frac{233}{128} + \frac{3}{8}\zeta(3) - \frac{5}{64}\ln(4Z)\right) + \mathcal{O}\left(\frac{1}{Z^2}\right) , \\
\Pi_0^{(3),\mathrm{mv}} &= \frac{4298785}{124416} - \frac{3799}{864}\zeta(3) - \frac{145}{36}\zeta(5) + n_l\left(-\frac{64627}{31104} - \frac{1}{216}\zeta(3)\right) \\
&\quad + \frac{1}{Z}\left\{-\frac{187715}{6912} + \frac{79355}{18432}\ln(4Z) - \frac{3127}{6144}\ln^2(4Z) + \zeta(2) + \frac{1}{3}\zeta(2)\ln 2\right. \\
&\quad -\frac{349853}{27648}\zeta(3) + \frac{15}{128}\zeta(3)\ln(4Z) + \frac{81}{64}\zeta(4) + \frac{23425}{3456}\zeta(5) + n_l\left[\frac{785}{576}\right. \\
&\quad \left.\left. -\frac{181}{1152}\ln(4Z) + \frac{11}{384}\ln^2(4Z) - \frac{1}{6}\zeta(2) + \frac{89}{96}\zeta(3)\right]\right\} + \mathcal{O}\left(\frac{1}{Z^2}\right) . \qquad (24)
\end{aligned}
$$

The small- and large-$Z$ expansions of the MOM $\beta$ function read:

$$
\begin{aligned}
\beta_0^{\mathrm{MOM}} &\underset{Z\to 0}{=\!=} \frac{11}{4} - \frac{n_l}{6} - Z\frac{2}{15} + \mathcal{O}\left(Z^2\right) , \\
\beta_1^{\mathrm{MOM}} &\underset{Z\to 0}{=\!=} \frac{51}{8} - n_l\frac{19}{24} + Z\left(\frac{4879}{97200} - \frac{7}{15}\ln(4Z)\right) + \mathcal{O}\left(Z^2\right) , \\
\beta_2^{\mathrm{MOM}} &\underset{Z\to 0}{=\!=} \frac{27045}{512} - \frac{5643}{512}\zeta(3) - n_l\left[\frac{7175}{768} - \frac{337}{768}\zeta(3)\right] + n_l^2\left[\frac{953}{3456} + \frac{1}{72}\zeta(3)\right] \\
&\quad + Z\left\{\frac{5640101219}{279936000} + \frac{995773}{1555200}\ln(4Z) - \frac{11269}{7680}\ln^2(4Z) - \frac{8}{15}\zeta(2)\right. \\
&\quad -\frac{8}{45}\zeta(2)\ln 2 - \frac{625415}{31104}\zeta(3) + n_l\left[\frac{1063}{87480} + \frac{305}{5832}\ln(4Z)\right. \\
&\quad \left.\left. +\frac{61}{2592}\ln^2(4Z) + \frac{4}{45}\zeta(2)\right]\right\} + \mathcal{O}\left(Z^2\right) , \qquad (25)
\end{aligned}
$$

$$
\begin{aligned}
\beta_0^{\rm MOM} &\underset{Z\to\infty}{=\!=} \frac{31}{12} - \frac{n_l}{6} + \frac{1}{4Z} + \mathcal{O}\left(\frac{1}{Z^2}\right), \\
\beta_1^{\rm MOM} &\underset{Z\to\infty}{=\!=} \frac{67}{12} - n_l\,\frac{19}{24} + \frac{1}{Z}\left(\frac{243}{128} - \frac{5}{64}\ln(4Z) + \frac{3}{8}\zeta(3)\right) + \mathcal{O}\left(\frac{1}{Z^2}\right), \\
\beta_2^{\rm MOM} &\underset{Z\to\infty}{=\!=} \frac{604877}{13824} - \frac{48701}{4608}\,\zeta(3) + n_l\left[-\frac{60763}{6912} + \frac{1075}{2304}\,\zeta(3)\right] + n_l^2\left[\frac{953}{3456} + \frac{1}{72}\,\zeta(3)\right] \\
&\quad + \frac{1}{Z}\left\{\frac{751727}{27648} - \frac{32029}{6144}\,\ln(4Z) + \frac{3127}{6144}\,\ln^2(4Z) - \zeta(2) - \frac{1}{3}\,\zeta(2)\,\ln 2\right. \\
&\quad + \frac{338477}{27648}\,\zeta(3) - \frac{15}{128}\,\zeta(3)\,\ln(4Z) - \frac{81}{64}\,\zeta(4) - \frac{23425}{3456}\,\zeta(5) + n_l\left[-\frac{1265}{1152}\right. \\
&\quad \left.\left. + \frac{79}{384}\,\ln(4Z) - \frac{11}{384}\,\ln^2(4Z) + \frac{1}{6}\,\zeta(2) - \frac{85}{96}\,\zeta(3)\right]\right\} + \mathcal{O}\left(\frac{1}{Z^2}\right). \qquad (26)
\end{aligned}
$$

Note that our result for the MOM $\beta$ function explicitly demonstrates the validity of the Applelquist-Carazonne theorem [27] at the three-loop level. Indeed, one can easily check that, for $i = 0, 1$ and 2, one has

$$
\begin{aligned}
\lim_{Z\to 0} \beta_i^{\rm MOM} &\equiv \beta_{i,\rm ml}^{\rm MOM}(n_f = n_l), \\
\lim_{Z\to \infty} \beta_i^{\rm MOM} &\equiv \beta_{i,\rm ml}^{\rm MOM}(n_f = n_l + 1),
\end{aligned}
$$

where $\beta_{i,\rm ml}^{\rm MOM}(n_f)$ is the three-loop contribution to the MOM $\beta$ function in the massless limit (see Eq. (8)).

In Fig. 2, we present the results for the MOM $\beta$ function in graphical form, where the one-, two- and three-loop coefficients are shown as functions of $Z$ in the Euclidian region. Next to the low- and high-energy approximations (dashes) including the $Z^3$ and $1/Z^5$ terms, also the interpolation functions (dotted) are shown. At the one- and two-loop orders, these results are compared against the exact result (solid line). For demonstration purpose, we have chosen $n_l = 5$ at the three-loop order. Very similar results are obtained for other values of $n_l$.

# 4 Phenomenological applications

In the following, we discuss the numerical impact of the results obtained in this paper. In particular, we consider the $\overline{\rm MS}$ quantity $\alpha_s^{(5)}(M_Z)$ as input value and evaluate the strong coupling at lower and higher energy scales with different numbers of active flavours. On the one hand, this can be done in the $\overline{\rm MS}$ scheme applying the usual running and decoupling procedure (see, e.g., Refs. [8, 28]). In this case, one has to specify a scale $\mu_Q$ where the heavy quark $Q$ is integrated out. On the other hand, it is possible to switch from the $\overline{\rm MS}$ to the MOM ($\overline{\rm MOM}$) scheme for $\mu = M_Z$ and perform the running with the help of the MOM ($\overline{\rm MOM}$) $\beta$ function. The results obtained at lower and higher energies

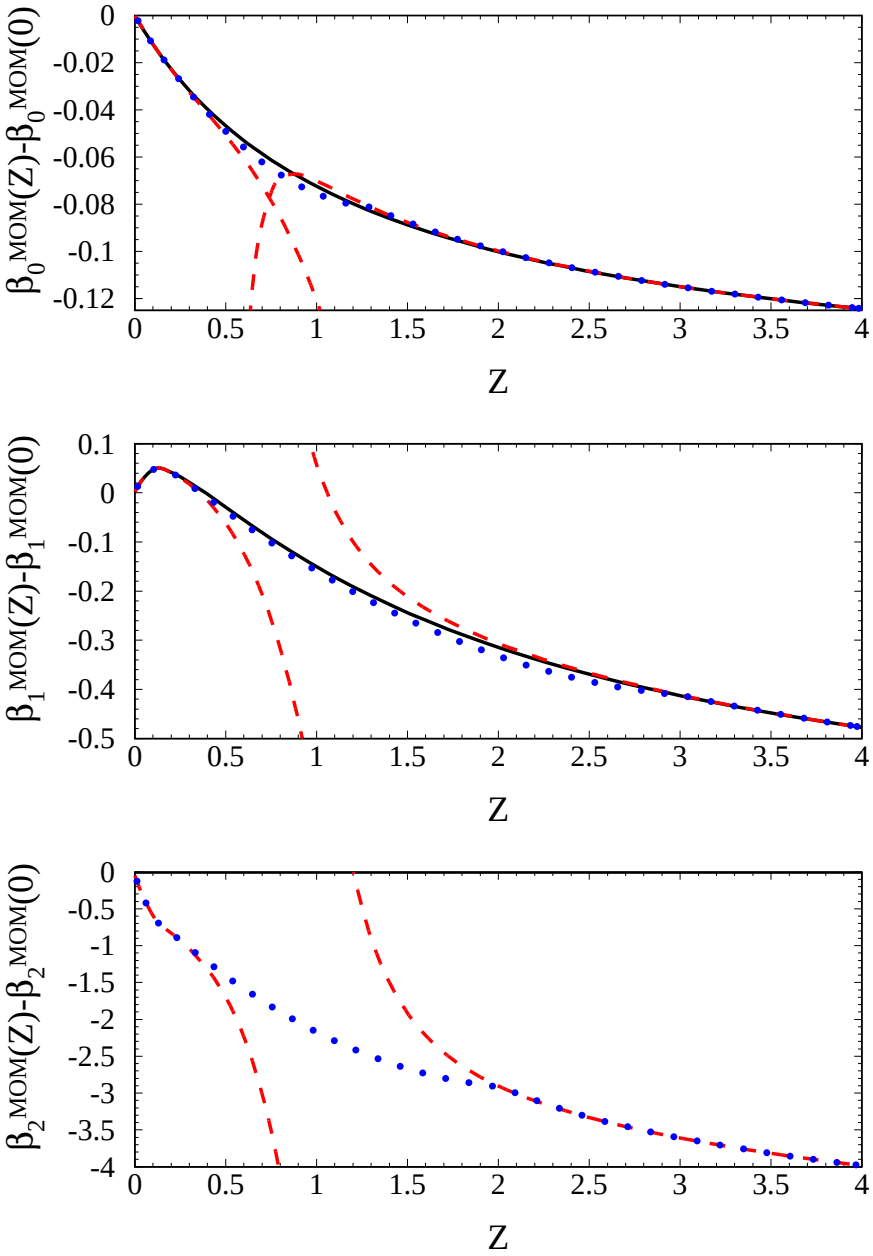


Figure 2: The difference $\beta_i^{\rm MOM}(Z) - \beta_i^{\rm MOM}(0)$ $(i = 0, 1, 2)$ as a function of $Z$ in the Euclidian region. In the three-loop result, $n_l = n_f - 1 = 5$ has been chosen. In each frame, the dashed lines represent the approximation for small and large values of $Z$, the dotted curve is the result of the interpolation, and the solid line (for $\beta_0^{\rm MOM}$ and $\beta_1^{\rm MOM}$) is the exact result from Ref. [11].

| $\mu$ (GeV) | $n_f$ | $\alpha_s^{(n_f)}(\mu)$ | | $n_f^{\rm MOM}$ | $\alpha_s^{\rm MOM}(\mu)$ | | $\alpha_s^{\rm MOM}(\alpha_s(\mu))$ | |
|---|---|---|---|---|---|---|---|---|
| | | 2 loop | 3 loop | | 2 loop | 3 loop | 2 loop | 3 loop |
| 91.19 | 5 | 0.1180 | 0.1180 | 6 | 0.1324 | 0.1331 | 0.1324 | 0.1331 |
| 200 | 5 | 0.1055 | 0.1055 | 6 | 0.1170 | 0.1175 | 0.1171 | 0.1175 |
| 350 | 6 | 0.0989 | 0.0990 | 6 | 0.1082 | 0.1086 | 0.1084 | 0.1087 |
| 500 | 6 | 0.0950 | 0.0951 | 6 | 0.1034 | 0.1037 | 0.1036 | 0.1038 |
| 1000 | 6 | 0.0884 | 0.0885 | 6 | 0.0953 | 0.0956 | 0.0955 | 0.0957 |

Table 1: $\alpha_s$ and $\alpha_s^{\rm MOM}$ for various values of $\mu$ from region A. As input, $\alpha_s(M_Z) = 0.118$ is used, which is transformed with the help of Eq. (4) to $\alpha_s^{\rm MOM}(M_Z)$. The running to different values of $\mu$ is achieved with the help of the appropriate $\beta$ function. $\alpha_s^{\rm MOM}(\alpha_s(\mu))$ is obtained from $\alpha_s(\mu)$ using Eq. (4).

| $\mu$ (GeV) | $n_f$ | $\alpha_s^{(n_f)}(\mu)$ | | $n_f^{\rm MOM}$ | $\alpha_s^{\overline{\rm MOM}}(\mu)$ | | $\alpha_s^{\overline{\rm MOM}}(\alpha_s(\mu))$ | |
|---|---|---|---|---|---|---|---|---|
| | | 2 loop | 3 loop | | 2 loop | 3 loop | 2 loop | 3 loop |
| 91.19 | 5 | 0.1180 | 0.1180 | 6 | 0.1192 | 0.1196 | 0.1192 | 0.1196 |
| 200 | 5 | 0.1055 | 0.1055 | 6 | 0.1066 | 0.1068 | 0.1066 | 0.1068 |
| 350 | 6 | 0.0989 | 0.0990 | 6 | 0.0993 | 0.0995 | 0.0993 | 0.0995 |
| 500 | 6 | 0.0950 | 0.0951 | 6 | 0.0952 | 0.0954 | 0.0952 | 0.0954 |
| 1000 | 6 | 0.0884 | 0.0885 | 6 | 0.0884 | 0.0885 | 0.0884 | 0.0885 |

Table 2: $\alpha_s$ and $\alpha_s^{\overline{\rm MOM}}$ for various values of $\mu$ from region A. As input, $\alpha_s(M_Z) = 0.118$ is used, which is transformed with the help of Eq. (13) to $\alpha_s^{\overline{\rm MOM}}(M_Z)$. The running to different values of $\mu$ is achieved with the help of the appropriate $\beta$ function. $\alpha_s^{\overline{\rm MOM}}(\alpha_s(\mu))$ is obtained from $\alpha_s(\mu)$ using Eq. (13).

can also be translated back to the $\overline{\rm MS}$ scheme, and a comparison can be performed. In this way, we can check the consistency between the two renormalization schemes.

For our numerical analysis, we use the following input values

$$\alpha_s^{(5)}(M_Z) = 0.118\,, \quad M_b = 4.7\ {\rm GeV}\,, \quad M_t = 175\ {\rm GeV}\,, \tag{27}$$

where $M_Q$ represent the pole quark masses and for the decoupling scales we choose $\mu_Q = 2\,M_Q$. The running and decoupling in the $\overline{\rm MS}$ scheme is performed with the help of `RunDec` [29].

We consider two regions of energies. Region A starts from the $Z$-boson mass, $M_Z$, and extends to energies much higher than the top-quark mass, say, 1000 GeV. In this region, we investigate the evolution of the strong-coupling constant in the MOM and $\overline{\rm MOM}$ schemes with five massless and one heavy quark, the top quark. Thus in total six quarks are present in the theory which we denote as $n_f^{\rm MOM} = 6$. On the other hand, in region B, we consider the evolution of $\alpha_s^{\rm MOM}(\mu)$ and $\alpha_s^{\overline{\rm MOM}}(\mu)$ from $\mu = M_Z$ down to $\mu = 3$ GeV. The number of massless quarks for region B is set to four, and the heavy quark be should identified with the bottom quark, i.e., we have $n_f^{\rm MOM} = 5$.

| $\mu$ (GeV) | $n_f$ | $\alpha_s^{(n_f)}(\mu)$ | | $n_f^{\rm MOM}$ | $\alpha_s^{\rm MOM}(\mu)$ | | $\alpha_s^{\rm MOM}(\alpha_s(\mu))$ | |
|---|---|---|---|---|---|---|---|---|
| | | 2 loop | 3 loop | | 2 loop | 3 loop | 2 loop | 3 loop |
| 91.19 | 5 | 0.1180 | 0.1180 | 5 | 0.1328 | 0.1332 | 0.1328 | 0.1332 |
| 50 | 5 | 0.1298 | 0.1298 | 5 | 0.1480 | 0.1486 | 0.1480 | 0.1486 |
| 10 | 5 | 0.1779 | 0.1781 | 5 | 0.2177 | 0.2198 | 0.2160 | 0.2192 |
| 4 | 4 | 0.2288 | 0.2287 | 5 | 0.3074 | 0.3148 | 0.2988 | 0.3096 |
| 3 | 4 | 0.2536 | 0.2538 | 5 | 0.3556 | 0.3682 | 0.3404 | 0.3574 |

Table 3: $\alpha_s$ and $\alpha_s^{\rm MOM}$ for various values of $\mu$ from region B. As input, $\alpha_s(M_Z) = 0.118$ is used, which is transformed with the help of Eq. (4) to $\alpha_s^{\rm MOM}(M_Z)$. The running to different values of $\mu$ is achieved with the help of the appropriate $\beta$ function. $\alpha_s^{\rm MOM}(\alpha_s(\mu))$ is obtained from $\alpha_s(\mu)$ using Eq. (4).

| $\mu$ (GeV) | $n_f$ | $\alpha_s^{(n_f)}(\mu)$ | | $n_f^{\rm MOM}$ | $\alpha_s^{\overline{\rm MOM}}(\mu)$ | | $\alpha_s^{\overline{\rm MOM}}(\alpha_s(\mu))$ | |
|---|---|---|---|---|---|---|---|---|
| | | 2 loop | 3 loop | | 2 loop | 3 loop | 2 loop | 3 loop |
| 91.19 | 5 | 0.1180 | 0.1180 | 5 | 0.1180 | 0.1181 | 0.1180 | 0.1181 |
| 50 | 5 | 0.1298 | 0.1298 | 5 | 0.1298 | 0.1300 | 0.1298 | 0.1300 |
| 10 | 5 | 0.1779 | 0.1781 | 5 | 0.1797 | 0.1804 | 0.1798 | 0.1807 |
| 4 | 4 | 0.2288 | 0.2287 | 5 | 0.2350 | 0.2376 | 0.2352 | 0.2385 |
| 3 | 4 | 0.2536 | 0.2538 | 5 | 0.2612 | 0.2652 | 0.2615 | 0.2667 |

Table 4: $\alpha_s$ and $\alpha_s^{\overline{\rm MOM}}$ for various values of $\mu$ from region B. As input, $\alpha_s(M_Z) = 0.118$ is used, which is transformed with the help of Eq. (13) to $\alpha_s^{\overline{\rm MOM}}(M_Z)$. The running to different values of $\mu$ is achieved with the help of the appropriate $\beta$ function. $\alpha_s^{\overline{\rm MOM}}(\alpha_s(\mu))$ is obtained from $\alpha_s(\mu)$ using Eq. (13).

In Tab. 1, we compare the values for $\alpha_s$ for some selected $\mu$ values from region A in the $\overline{\rm MS}$ and MOM schemes. For all numbers, we choose $\alpha_s^{(5)}(M_Z)$ as the starting point, transform at $\mu = M_Z$ to the MOM scheme and use the corresponding renormalization group equation to arrive at the desired $\mu$ values. The same comparison for the case of the $\overline{\rm MOM}$ scheme is shown Tab. 2. In both tables, we show in the last two columns the results of $\alpha_s^{\rm MOM}(\mu)$ (Tab. 1) and $\alpha_s^{\overline{\rm MOM}}(\mu)$ (Tab. 2) as obtained from the $\overline{\rm MS}$-evolved value $\alpha_s(\mu)$ using Eqs. (4) and (13), respectively. The corresponding results for region B are shown in Tabs. 3 and 4 (where, of course, the values given in Eq. (19) have been used).

All four tables show good agreement between the values of the MOM coupling constant obtained via direct integration of the (quark-mass-dependent) MOM $\beta$ function and with the help of the (simpler) conversion from the $\overline{\rm MS}$ scheme. For Tabs. 1 and 3 the agreement is even getting better after taking into account the three-loop corrections. Note that the results in the case of the $\overline{\rm MOM}$ scheme become slightly worse after switching on the three-loop terms, as can be seen in Tabs. 2 and 4. The reason for this can be seen by comparing Eq. (16) with Eq. (10). The former has (by construction) vanishing order $\alpha_s$ corrections and a two-loop coefficient which is smaller by a factor of six. However, the three-loop

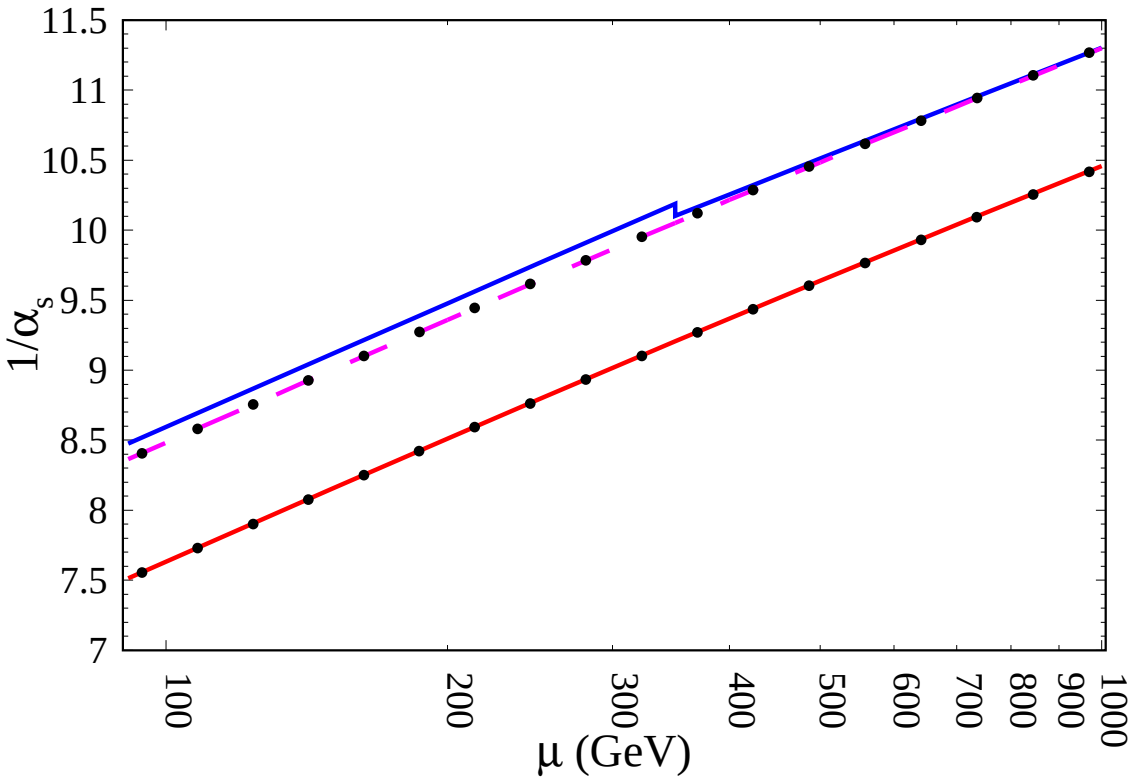


Figure 3: $1/\alpha_s$ as a function of $\mu$. The (blue) upper solid line containing a step for $\mu = 2M_t$ corresponds to the $\overline{\rm MS}$ result and the (red) lower solid line to the result in the MOM scheme. The (pink) dashed line represents $1/\alpha_s$ in the $\overline{\rm MOM}$ scheme. The (black) dotted lines lying on top of the MOM and $\overline{\rm MOM}$ result correspond to the results obtained from $\overline{\rm MS}$ value of $\alpha_s$ using the conversion formulae (4) and (13), respectively. For all results the three-loop expressions have been used and $n_f^{\rm MOM} = 6$ has been chosen.

term is only reduced by a factor of three and thus has bigger relative influence. Still, the difference between $\alpha_s^{\overline{\rm MOM}}(\mu)$ and $\alpha_s^{\overline{\rm MOM}}(\alpha_s(\mu))$ for $\mu = 3$ GeV is about a factor of ten less than the current best value obtained, e.g., from hadronic $\tau$ decay (see, e.g., Ref. [30]).

In Figs. 3 and 4, the results of Tabs. 1–4 are shown in graphical from. In particular, we plot the inverse strong coupling as a function of $\mu$ both for the $\overline{\rm MS}$, MOM and $\overline{\rm MOM}$ schemes, where in all cases the three-loop approximation is used for the running and the conversion between the schemes. We again choose $\alpha_s^{(5)}(M_Z)$ as the input quantity and convert at this scale to the other two schemes. The evolution of the $\overline{\rm MS}$ coupling to lower $\mu$ values is shown by the (upper) solid lines with a step at the values for $\mu_t = 2M_t$ and $\mu_b = 2M_b$, respectively. Numerically very close is the dashed curve in the $\overline{\rm MOM}$ scheme, which is expected from the above discussion. The lower solid line represents the result in the MOM scheme. Both for the MOM and $\overline{\rm MOM}$ results, the conversion is performed for $\mu = M_Z$, and the running to other values of $\mu$ is achieved using the corresponding $\beta$

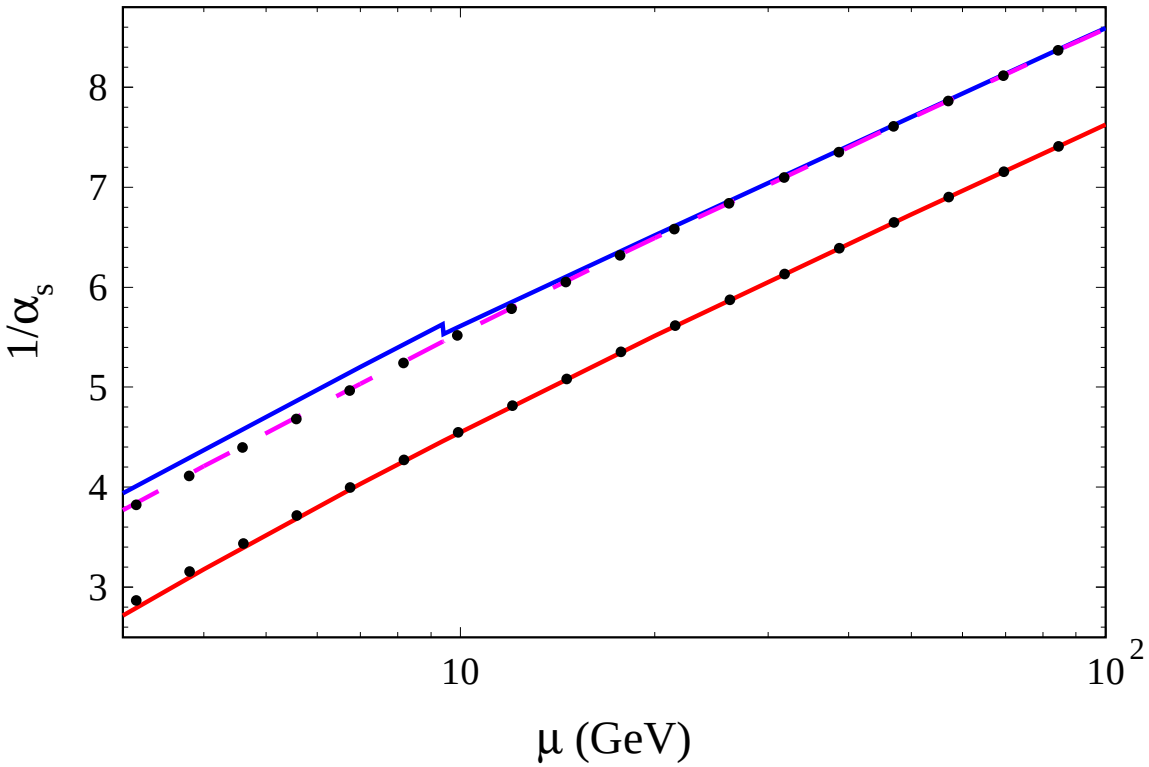


Figure 4: The same coding as in Fig. 3 has been adapted, except that $n_f^{\rm MOM} = 5$ has been chosen.

function. The dotted lines on top of the MOM and $\overline{\rm MOM}$ curves represent the results where the transformation from the $\overline{\rm MS}$ values is performed just at the considered value of $\mu$.

# 5 Conclusions

We have computed the three-loop corrections to the $\beta$ function of QCD with one heavy and $n_l$ massless quarks in a momentum subtraction scheme (MOM). In our three-loop calculation, we do not consider the diagrams involving two different quark masses. Although there are only a few diagrams of this type, their evaluation is significantly more difficult.

We have shown that our results describe the MOM coupling constant evolution in well-defined kinematical regions with three-loop accuracy. Moreover, the numerical analysis of our results has clearly demonstrated the full equivalence of the schemes with explicitly built-in decoupling (MOM and $\overline{\rm MOM}$) to the standard $\overline{\rm MS}$ scheme, which, as is well-known, does not have such a property.

From the more technical point of view, it has been shown that one can use the $\overline{\rm MS}$

scheme evolution along with simple conversion relations (derived for the regions either significantly above or below the heavy-quark threshold) to relate the values of the MOM scheme coupling constant from both regions.

Finally, we believe that our analysis should help to remove the last traces of doubt about the usefulness of $\overline{\rm MS}$-like schemes, which formally do not obey the the Applelquist-Carazzone theorem [27], for a unified description of mass effects in a broad region of $\mu^2$ values, from far below heavy-quark thresholds to well beyond them.

## Acknowledgments

This work was supported in part by the BMBF through Grant Nos. 05 HT6VKA and 05 HT6GUA and by the DFG through SFB/TR 9.

# References

[1] G. 't Hooft, Nucl. Phys. B **61** (1973) 455.

[2] W. A. Bardeen, A. J. Buras, D. W. Duke and T. Muta, Phys. Rev. D **18** (1978) 3998.

[3] G. 't Hooft and M. J. G. Veltman, Nucl. Phys. B **44** (1972) 189.

[4] J. F. Ashmore, Lett. Nuovo Cim. **4** (1972) 289.

[5] G. M. Cicuta and E. Montaldi, Lett. Nuovo Cim. **4** (1972) 329.

[6] J. A. M. Vermaseren, S. A. Larin and T. van Ritbergen, Phys. Lett. B **405** (1997) 327 [hep-ph/9703284].

[7] M. Czakon, Nucl. Phys. B **710** (2005) 485 [hep-ph/0411261].

[8] K. G. Chetyrkin, B. A. Kniehl and M. Steinhauser, Nucl. Phys. B **510** (1998) 61 [arXiv:hep-ph/9708255].

[9] Y. Schröder and M. Steinhauser, JHEP **0601** (2006) 051 [arXiv:hep-ph/0512058].

[10] K. G. Chetyrkin, J. H. Kühn and C. Sturm, Nucl. Phys. B **744** (2006) 121 [arXiv:hep-ph/0512060].

[11] F. Jegerlehner and O. V. Tarasov, Nucl. Phys. B **549** (1999) 481 [arXiv:hep-ph/9809485].

[12] L. F. Abbott, Nucl. Phys. B **185** (1981) 189.

[13] N. N. Bogolyubov and D. V. Shirkov, Nuovo Cim. **3** (1956) 845.

[14] D. V. Shirkov, hep-th/9903073.

[15] O. V. Tarasov, A. A. Vladimirov and A. Y. Zharkov, Phys. Lett. B **93** (1980) 429.

[16] S. A. Larin and J. A. M. Vermaseren, Phys. Lett. B **303** (1993) 334 [arXiv:hep-ph/9302208].

[17] D. Binosi and L. Theussl, Comput. Phys. Commun. **161** (2004) 76 [arXiv:hep-ph/0309015].

[18] J. A. M. Vermaseren, Comput. Phys. Commun. **83** (1994) 45.

[19] S. G. Gorishnii, S. A. Larin, L. R. Surguladze and F. V. Tkachov, Comput. Phys. Commun. **55** (1989) 381.

[20] S. A. Larin, F. V. Tkachov and J. A. M. Vermaseren, preprint NIKHEF-H-91-18 (1991).

[21] P. Nogueira, J. Comput. Phys. **105** (1993) 279.

[22] J. A. M. Vermaseren, arXiv:math-ph/0010025.

[23] R. Harlander, T. Seidensticker and M. Steinhauser, Phys. Lett. B **426** (1998) 125 [hep-ph/9712228].

[24] T. Seidensticker, hep-ph/9905298.

[25] V. A. Smirnov, "Applied asymptotic expansions in momenta and masses," Springer Tracts Mod. Phys. **177** (2002) 1.

[26] M. Steinhauser, Comput. Phys. Commun. **134** (2001) 335 [arXiv:hep-ph/0009029].

[27] T. Appelquist and J. Carazzone, Phys. Rev. D **11** (1975) 2856.

[28] M. Steinhauser, Phys. Rept. **364** (2002) 247 [arXiv:hep-ph/0201075].

[29] K. G. Chetyrkin, J. H. Kühn and M. Steinhauser, Comput. Phys. Commun. **133** (2000) 43 [arXiv:hep-ph/0004189].

[30] P. A. Baikov, K. G. Chetyrkin and J. H. Kühn, Phys. Rev. Lett. **101** (2008) 012002 [arXiv:0801.1821 [hep-ph]].